Linseed oil-filled microcapsules containing drier and corrosion inhibitor – their effect on self-healing

Tamás Szabó[a*], Judit Telegdi[a,b], Lajos Nyikos[a]

[a]Functional Interfaces Research Group, Institute of Materials and Environmental Chemistry, Research Centre for Natural Sciences, Hungarian Academy of Sciences, Magyar tudósok körútja 2., Budapest, H-1117 Hungary
[b]Óbuda University, Rejtő Sándor Faculty of Light Industry and Environmental Engineer, Institute of Media-technology and Light Industry; Doberdó út 6. Budapest, H-1034 Hungary
[*]corresponding author, e-mail: szabo.84.tamas@ttk.mta.hu, tel.: +36 1 438-1100 / 545

Abstract
Core-shell microcapsules of urea-resorcinol-formaldehyde shell and linseed oil (LO) core material as paint additives for self-healing coatings were prepared. The capsules contained LO either with or without Co-octoate as drier material and/or octadecylamine (ODA) as corrosion inhibitor. The microcapsules embedded in a commercial paint were applied on sandblasted mild steel sheets. After scratching the coated surface, the inhibition efficiency of core-shell microcapsule-containing coat, dipped into corrosive media, was followed visually and evaluated numerically by electrochemical impedance spectroscopy (EIS). In separate experiments, to optimize for the self-healing process, the composition of the core material, the effect of the drier and/or the inhibitor ODA on drying process of LO films were monitored by infrared spectroscopy. Pure LO needed 6-7 days to dry completely. The drying period could be shortened (to 5 h) via application of a dryer, but the addition of the corrosion inhibitor alone increased significantly the time needed for solifidicaiton. To minimize the drying period we have found the proper combination of the ODA and the dryer of the LO.
The EIS measurements, in accordance with the drying tests, resulted in the next order of self-healing ability: $LO<LO_{(+ODA)}<LO_{(+Co-octoate)}<LO_{(+ODA+Co-octoate)}$.

Keywords

linseed oil, microcapsules, self-healing, inhibitor, octadecylamine

1. Introduction

Coatings of metals that can restore their sealing ability and show anti-corrosion profile after physical damage have a broad range of research directions.
Amongst these coating research there are two major classes. One direction is the study on re-organizable polymer coatings with the ability of molecular bonds curable via ultraviolet or infrared irradiation.
On the other hand researchers make huge effort to develop porous nano/microcarriers and core-shell capsules as paint additives, that, in case of mechanical decay, deliver corrosion inhibitors or liquid glue-like monomers which serve as sealant barrier between metallic surface and corrosive media. These two types were reviewed lately in details [1,2].
Both strategies have adventages and disadvantages. Porous nanoparticles provide inhibitive effect upon pH-change when damaged sites are in contact with humidity. There are cerium-based particles in carriers like chitosan [3], CeO_2 nanoparticles [4], hydroxyapatite- [5] and $CaCO_3$ [6] microparticles; mercaptobenzothiazole in layered double hydroxides [7] and polyelectrolyte nanocapsules [8] as well as benzotriazole in mesoporous silica particles [9].

Nanoparticles in general do not weaken significantly the mechanical properties and permeability of coatings [7,10,11,12], but their inhibition lasts only until the depletion of the nanocarriers. In contrast to it, core-shell capsules with special core materials form a novel insulating coating layer that prevent further connections to corrosive media. The mechanical properties of the microcapsules-embedded coatings are somewhat weaker according to pull-off- [13], adhesion- [14] or tensile tests [15].

In the literature there are several papers on preparation of core-shell microcapsules with various core materials: linseed oil [13,15,16,17,18,19,20], tung oil [21], two-component epoxy hardeners [22], water reactive silyl esters [23], methyl methacrylate [24], dicyclopentadiene [23,25,26,27] etc. are mentioned as the most important techniques. Mostly polycondensed polymers as shell materials are chosen like urea-formaldehyde [23,25,26,27,28], melamine-urea-formaldehyde [29].

Combination of these two strategies appeared in the literature, where CeO_2 and Cr_2O_3 nanoparticles as corrosion inhibitors were co-encapsulated with linseed oil as healing material [30].

When materials as film formers and anticorrosion additives are considered, amines are preferred as inhibitors due to their affinity to the steel surfaces like triethanolamine [31]. Compounds with smaller molecular weight are directly combined with paints, and in the last years some others like triethanolamine [32], dodecylamine [33], ethanolamine, diethanolamine, 5-amino-1-pentanol, propylamine, dipropylamine [34] are encaged in porous, slow-release micro- or nanoparticles.

Amines with longer carbon chains, e.g. octadecylamine form superhydrophobic insulating layer thus they can be applied even in harsh circumstances like high-temperature steam tanks, pipes, etc. [35,36].

Attempts were made to use ODA mixed directly in coating, but due to its hydrophobicity, first it had to be intorduced into an amphiphilic carrier, this was the ring-like, thoroid shaped β-cyclodextrin [37].

Our research aimed the combined application of a film former self-healing material (linseed oil) as well as of a corroison inhibitor (octadecylamine) in the core of microcapsules which were used as additives in self-healing paint.

Another aim of this study was to elucidate the influence of special additives that can increase the rate of solidification of the film former linseed oil, can affect the self-healing ability, and could be built in the microcapsules, too.

2. Experimental

2.1. Materials

Used for encapsulation: linseed oil ('LO', Poli Farbe, raw); urea (Fluka, p.a.); resorcinol (Reanal, purum); formaldehyde (37% aqueous solution, Sigma-Aldrich, purum); ammonium-chloride (Reanal, purum); hydrochloric acid (10% solution, Reanal, a.r.); poly(vinyl alcohol) ('PVA', Sigma, purum); sodium-dodecylsulfate ('SDS', Sigma-Aldrich); ethanol (Molar Chemicals Kft., a.r.).
Other: sandblasted mild steel sheets (SB2½ grain size; atomic composition: Fe (88.6±0.7), C (10.8±0.6), Al (0.6±0.1) at%); dual function paint (vinyl polymer-type, primer and topcoat in one, ALVIKORR, Egrokorr Zrt.); octadecylamine ('ODA', Fluka, puriss); cobalt-octoate (drier, industrial grade); sodium chloride (Reanal, a.r.).

2.2. Preparation of microcapsules, coatings and linseed oil films

Our modified microcapsule preparation was based on the literature [16]. 10ml LO with Co-octoate (drier) and inhibitor ODA was dispersed in 100 ml 2% PVA solution which conatined 1.25 g urea, 0.125 g resorcinol and 0.125 g ammonium-chloride via stirring with 2000 rpm speed for 25 min. When the drier and inhibitor was introduced into LO, the aqueos phase contained 0.5% SDS surfactant. Into the homogenous dispersion 3.21 g formaldehyde solution was added. With continuous stirring, the reaction temperature was set to 70°C by 1°C/min heating speed and kept at this temperature for another 5 hours. After cooling down to room temperature, the microcapsules were washed with 50% aqueous ethanol, filtrated and dried under vacuum.

Microcapsules, prepared as described above, were mixed into the dual function (primer- and topcoat) paint in 5%, and this mixture was applied on sandblasted mild steel sheets. The thickness of the paint layers was 100 μm.

In order to investigate the drying process of the LO, in separate experiments 50 μl of LO was spread on one side of a glass (26x76 mm) slide. The thickness of the LO film was 0.025 mm which was comparable with the diameter of the microcapsules. Ten different compositions were tested. The LO was applied without any additive; with 1-, 2-, 3 and 5 v/v% Co-octoate alone or in combination with 2% ODA.

2.3. Infrared investigation of linseed oil films drying

Fourier transform infrared (FTIR) spectra of drying LO were recorded using attenuated total reflection (ATR) technique by means of a Varian 2000 (Scimitar Series) FTIR spectrometer (Varian Ltd, USA) equipped with nitrogen cooled MCT (mercury-cadmium telluride) detector and adjusted with a 'Golden Gate' (Specac Inc, UK) single reflection diamond ATR unit. Spectra were collected by co-addition of 128 individual interferograms with a spectral resolution of 4 cm^{-1}. Each spectrum was ATR corrected using the Varian Resolutions Pro 4.0 software package. The samples were mounted on the ATR crystal.

2.4. Visual and electrochemical characterization of paints with microcapsules

LO-filled microcapsules are visualized by scanning electronmicroscope ('SEM', Zeiss EVO 40 XVP).

For the corrosion test, the coated mild steel sheets were scratched with a blade, leaving 200 μm wide and 15 mm long, X-shaped scars. Around the cuts, glass rings were fastened with silica gel to form cells. The surface area was 3.8 cm^2. The cells were filled with corrosive, aerated 0.5 M NaCl solution.

Electrochemical impedance spectroscopy (EIS) measurements were carried out with a Zahner Im5d Impedance Spectrum Analyzer, at open circuit potential. The spectra were recorded in the frequency range of 10 mHz–100 kHz, using a sinusodial perturbation of 10 mV p–p amplitude. The measurements were started after 15 min of immersion in the corrosive media and spectra were collected in every hour during 24 h. The impedance spectra were evaluated with the Equivcrt software [38] by assuming a parallel combination of a charge transfer resistance and a dispersive double layer impedance (a constant phase element) with a simple series resistance. R1(R2Q) was found to adequately represent all the data. A standard three-electrode cell was used for the electrochemical measurements. The counter electrode was platinum. The electrode potential was measured against a saturated calomel electrode.

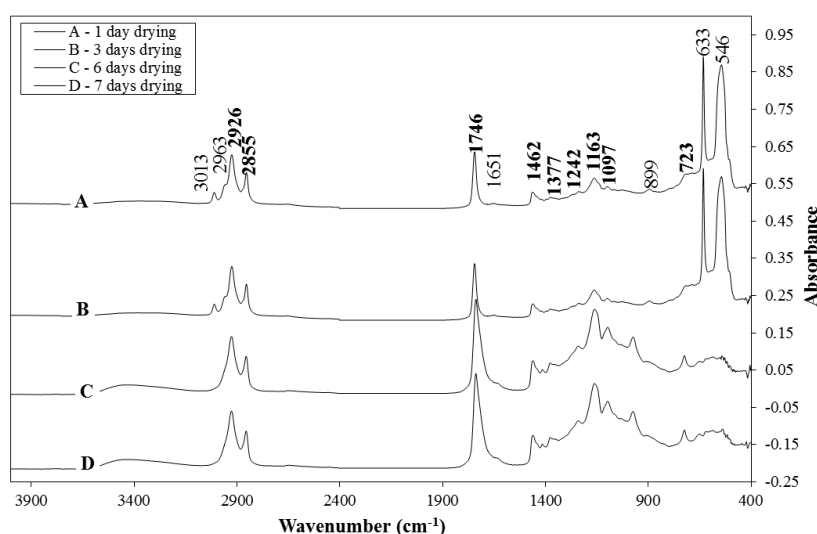## 3. Results and discussion

3.1. Drying of linseed oil films

Fig. 1. Changes in the FTIR spectra due to the drying process in the linseed oil film, A: after 1 day; B: after 3 days, C: after 6 days and D: after 7 days.
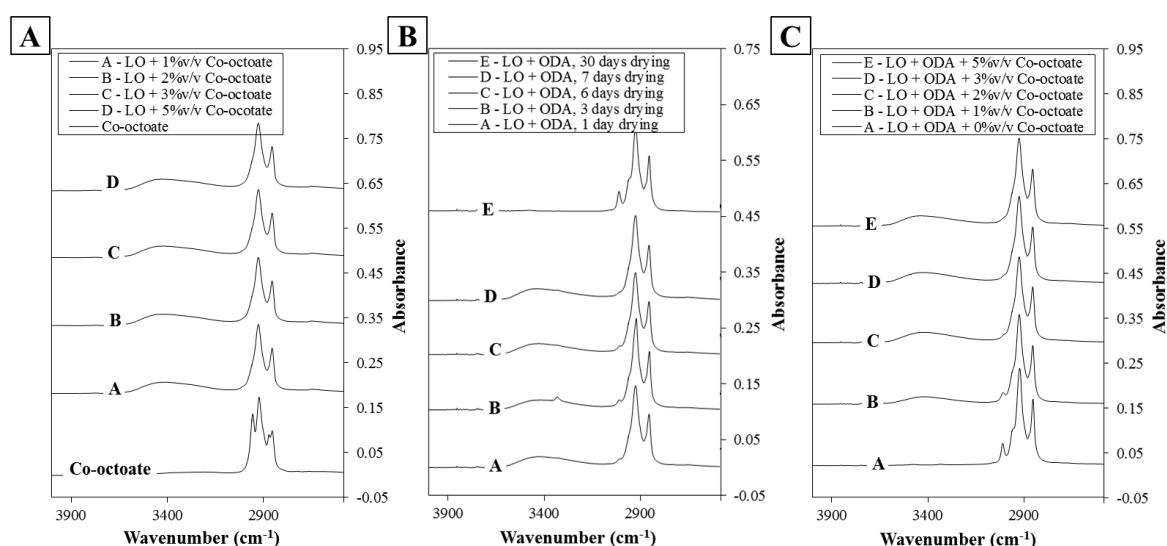

Fig. 2. FTIR spectral changes of drying linseed oil films. A: Drying of LO film in 5 h with different amounts of Co-octoate. B: influence of 2% ODA in the LO film on the drying process. C: Drying of LO film in 5 h, containing 2% ODA and different amounts of Co-octoate.

The IR spectra of pure linseed oil during the drying process were monitored for a week (Fig. 1.). Maxima of absorption bands found at 2855, 2926, 2963 and 3013 cm^{-1} can be assigned as υ_s(C–H)CH$_2$, υ_a(C–H)CH$_2$, υ_a(C–H)CH$_3$ és υ(C–H)=CH, respectively (υ_s: symmetrical stretching; υ_a: asymmetrical stretching) [39]. The latter C–H stretching belongs to the double-bond in the unsaturated alkyl chain of the glycerides. Its weakening and disappearence is the consequence of chemical reactions in the oxidative drying process of the linseed oil [39]. From the spectra on Fig. 1. one can see that after 3 days, the absorption band at 3013 cm^{-1} is still present, but after 7 days the shoulder totally vanishes, the oil has no traces of unsaturation.

There are no more significant changes in spectra helping to track the drying, with the exception of absorption bands at 633 and 546 cm^{-1}. Both of these bands' intensity decreased

and finally disappeared after the solidification of the LO film. However these bands belong to the sapphire crystal which ensures that the samples are downforced onto the ATR-diamond. When Co-octoate siccative was mixed into the LO film, the time of the total drying was reduced to several hours. The results are summarized in Fig. 2.A. The infrared spectra of LO films (A, B, C and D) represent the influence of the changing concentration of the Co-octate (1-, 2-, 3 and 5 v/v% respectively) recorded 5 h after the Co-octate addition. They all lack the 3013 cm^{-1} band, and at sampling it was obious that the LO films are in solid state.

In order to get a more efficient self-healing as well as anticorrosion ability, 2% corrosion inhibitor ODA was added to the LO. This concentration is almost the maximum that can be dissolved in LO at room temperature. Important question was how can the presence of ODA influence the solidification of the LO film? Spectra in Fig. 2.B follow the drying films of LO mixed with ODA. The peak at 3013 cm^{-1} can not help to define the state of drying. The LO film was not solid even after a month, its surface inhomogenously dried. This unexpected behaviour, caused by the presence of ODA, weakens the self-healing process. In order to overcome this undesired effect and to increase the oxidation of the LO, to the LO/ODA mixture different amounts of Co-octate were added in order to find the most proper core material composition which is able not only to dry faster but show an enhanced anticorrosion activity. Fig. 2.C shows the spectra of LO with 2% ODA which contained different amounts of Co-octate (A: 0-, B: 1-, C: 2-, D: 3 and E: 5 v/v%, respectively), 5 h after the ODA- and Co-octate addition and film drawing. With 0- or 1 v/v% Co-octate the LO/ODA film did not dry in the monitored interval, witnessed by the present υ(C–H)=CH shoulder on the spectrum A and B. Further increase in the Co-octate concentration (3-5 v/v%) helps in curing the LO, shown on C, D and E spectra.

3.2. Microcapsules and coatings; their efficiency evaluated by visualization and electrochemical impedance spectroscopy

All numerical results got in experiments on the drying process of LO were used in the preparation of core-shell microcapsules when the core contained mixed compositions: LO+Co-octate, LO+ODA, LO+ODA+Co-octate.

In the first set of experiments the microcapsules are shown as prepared and their use in the preliminary healing experiments.
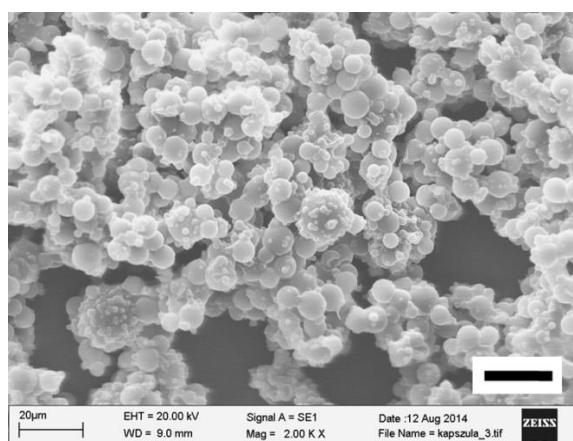

Fig. 3. SEM micrograph of LO-filled microcapsules. The scale represents 20 μm.

The microcapsules with LO core are illustrated with the SEM micrograph on Fig. 3. The surface of the capsules is smooth, their average diameter is 10±3 μm. The smaller objects on the picture are urea-formaldehyde polymeric particles.

After drying of the coatings which contained 5% microcapsules filled with LO, cuts were made on the surface (Fig. 4.A). The blade reached the metal surface, leaving a 200 μm wide wound. Some white particles appear along the scratching which originated from the paint. These coated and injured metals were dipped into the corrosive media. As the second photo (Fig. 4.B) shows, the microcapsules filled with LO were not enough to inhibit the corrosion after several days immersion. It was important to study the drying process of the LO in order to use the most porper conditions for the microcapsule preparation.
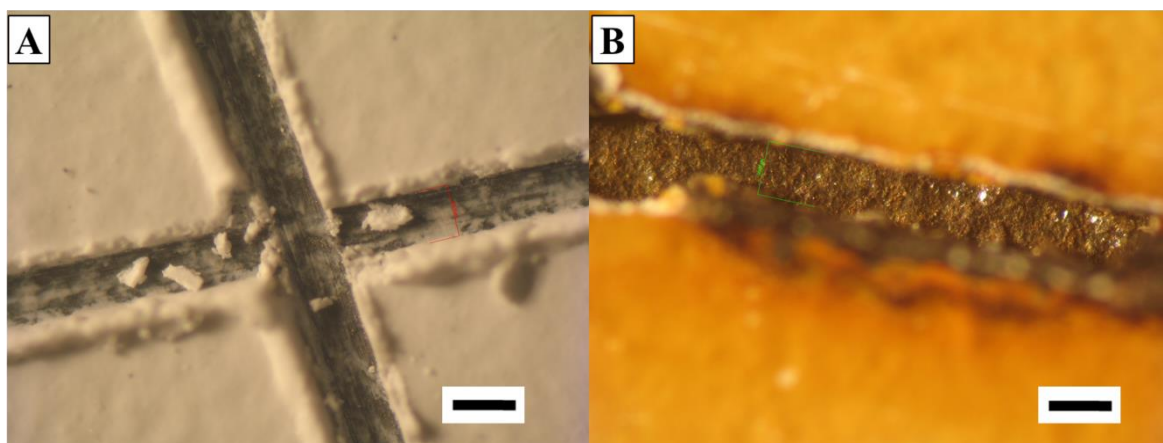

Fig. 4. Scratches cut in the coating, before immersion (A) and after the corrosion test (B). The scales represent 200 μm.

In more detailed experiments microcapsules were prepared when the core was filled with LO, LO/Co-octoate, LO/ODA and LO/Co-octoate/ODA and these particles were combined with paint and investigated in corrosion experiments.
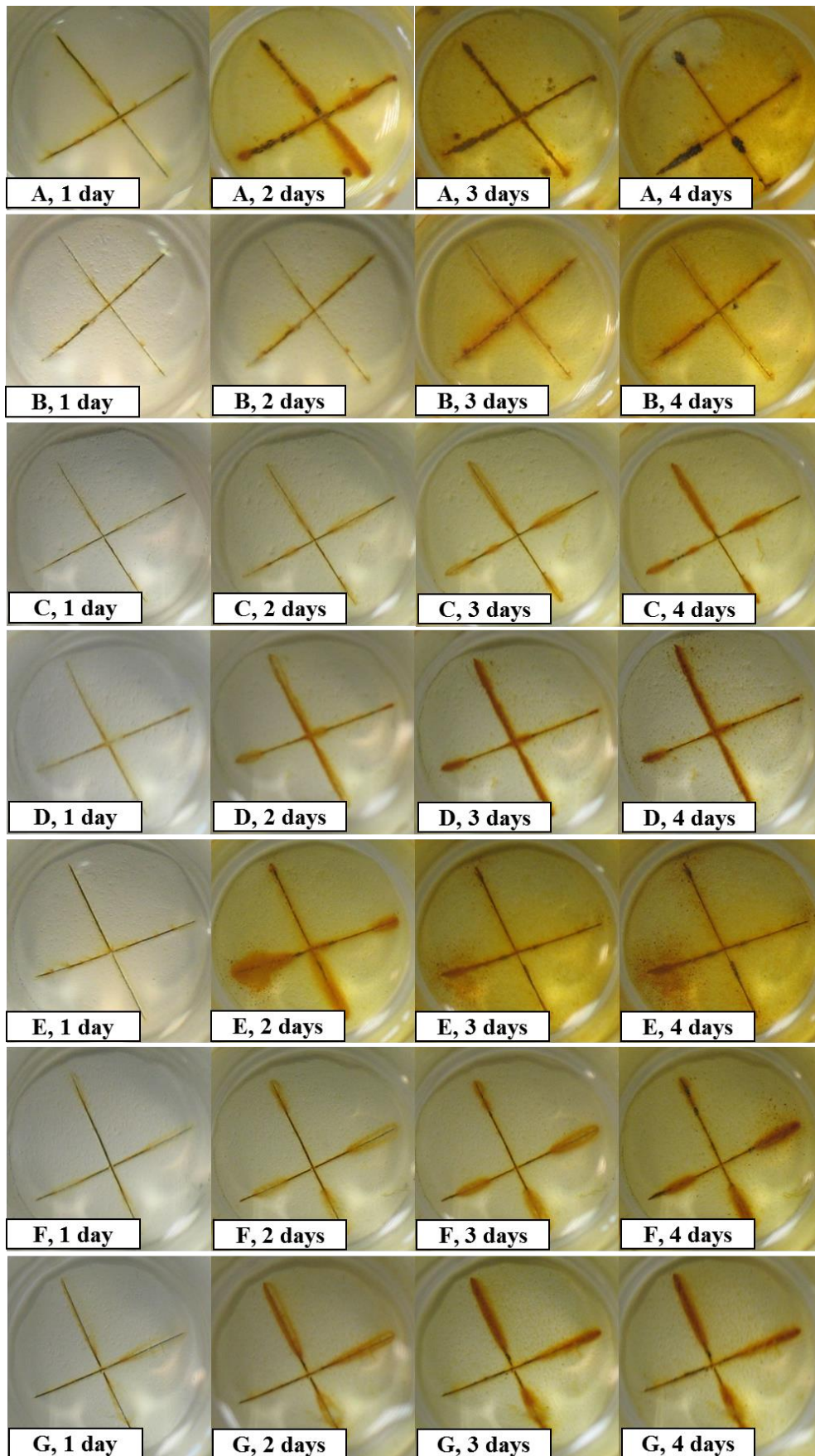
Fig. 5. Evolved corrosion of coated samples (A–G) in 0.5 M NaCl solution during 4 days, immersed different lapses after scratching. A: reference, without microcapsules, immersion

after 5 h. B: coating with LO-filled capsules, immersion after 5 h. C: coating with LO-filled capsules, immersion after 7 days. D: coating with LO + 1 v/v% Co-filled capsules, immersion after 5 h. E: coating with LO + 2% ODA-filled capsules, immersion after 5 h. F: coating with LO + 2% ODA-filled capsules, immersion after 7 days. G: coating with LO + 2% ODA + 2 v/v% Co-octoate-filled capsules, immersion after 5 h.

These core compositions listed in Table 1. were encapsulated and the microcapsules were added to paint in 5%. To evaluate their corrosion inhibiting efficiency, the painted and scratched surfaces were immersed into highly corrosive NaCl solution, with different lapses after the scarring. The corrosion phenomenon was followed visually for 4 days. The initial period of the coating degradation, which is very important in case of corrosion, was monitored in the first 24 h by electrochemical impedance spectroscopy.

The results of 4 day-long corrosion test are demonstrated in Fig. 5. The photos of experimental sets A–G show the oxidation of the scratched mild steel sheets coated previously with paint either with microencapsulated substances or without them. Table 1. summarizes the samples and lapses.

Table 1. Symbol of coated samples with different microcapsule-additives, their components and the lapses between the scratching of the coating and its immersion into electrolyte.

Sample ##	Lapse (hour/day)	Oil present (Yes/No)	Co-octoate (v/v%)	ODA (%)
A	5 h	N	–	–
B	5 h	Y	–	–
C	7 d	Y	–	–
D	5 h	Y	1	–
E	5 h	Y	–	2
F	7 d	Y	–	2
G	5 h	Y	2	2

The photos allow to evaluate the influence of microcapsules present in the coating, of the core materials, as well as of the drying time. It is obvious that in 4 days all of the samples suffered smaller or bigger degradation since the environment was very corrosive. The main aim was to optimize the core composition to get the best results.

The sample 'A' which represents the reference coating with no capsules, is highly corroded. Sample 'B', coating with microcapsules filled with LO shows some resistance, even without drying, as corrosion test with aqueous electrolyte started before the scratched coating was solid (according to the FTIR spectra). When the LO, after got free in the cutting, had 7 days to dry in the case of 'C', the self-healing worked more effectively than with sample 'B'; its efficiency was similar to that result got on sample 'D', where the LO's oxidation was helped with siccative (Co-octoate) but the drying time was much shorter, only 5 h. The presence of 2% ODA affected the inhibition negatively, the sheet corroded (E), almost as intensely as the reference sample. This could also be explained by the incomplete drying of the LO–ODA composition before coming in contact with the electrolyte. When the sample had time (7 days) to dry and only then was immersed in the corrosive solution, better corrosion resistance was observable (F). When in the core the LO contained 2% ODA and 2 v/v% drier, the drying was complete in 5 h, in accordance with the FTIR spectra. Though there is not significant difference between samples (F) and (G), the importance of a solidified surface is emphasized here. Curing of the LO can be achieved either by addition of siccative or by waiting for longer time, especially in presence of oxygen-consuming amines. For quantitative evaluation of the influence of microcapsules embedded in coatings four samples (A, B, D and G) were selected and characterized electrochemically.The EIS results are plotted on Fig. 6.A, B, D and G,

respectively. The complex impedance values of the samples are represented on Nyquist plots; 1-, 2-, 4-, 8- and 24 hours after immersion in each case.
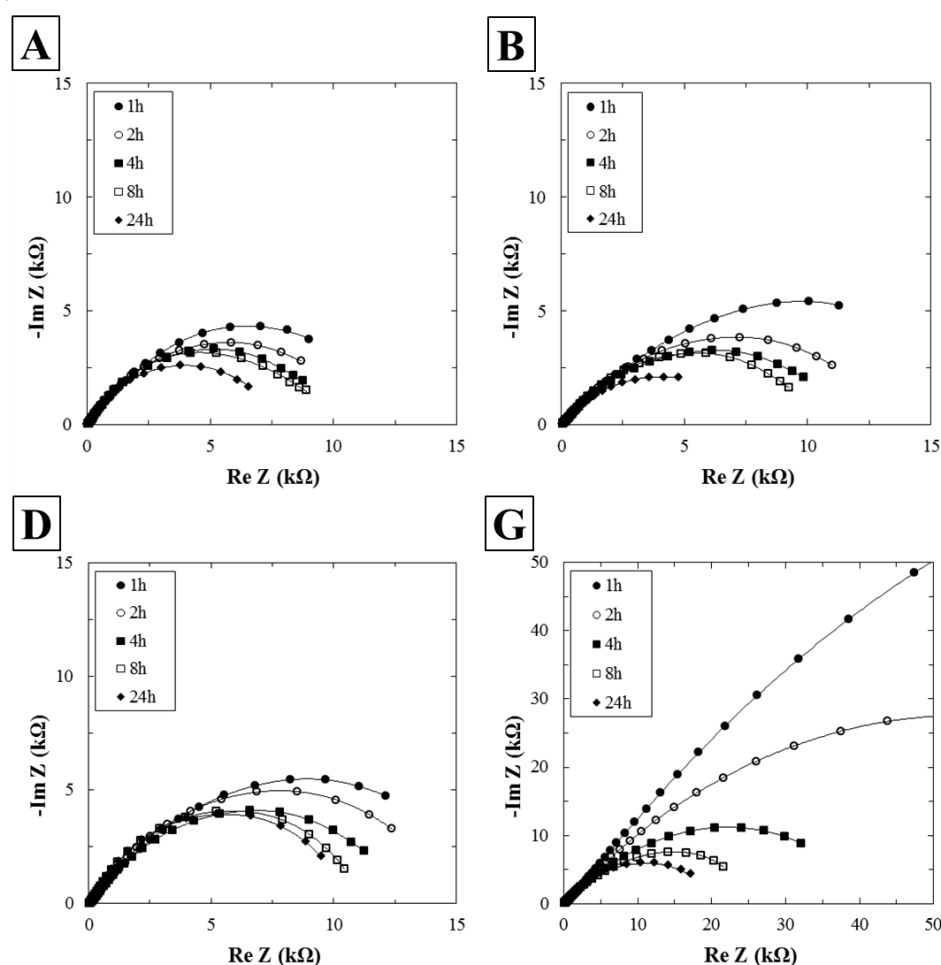

Fig. 6. Nyquist plots of scratched coatings, 1-($\bullet$), 2-($\circ$), 4-($\blacksquare$), 8-($\square$) and 24 hours ($\blacklozenge$) after immersion in 0.5 M NaCl solution. The samples are coated by paint: (A): with no capsules, (B): capsules with LO, (D): capsules with LO + 1 v/v% Co-octoate and (G): capsules with LO + 2% ODA + 2 v/v% Co-octoate.

From Nyquist plots, polarization resistance values (R_p) of all the samples were determined with software. These values which characterize the quality of coatings were calculated for the 1-, 4-, 8-, 12 and 24 h immersion times and are plotted on Fig. 7. All R_p curves show descending trend, with higher drop in the first hour.
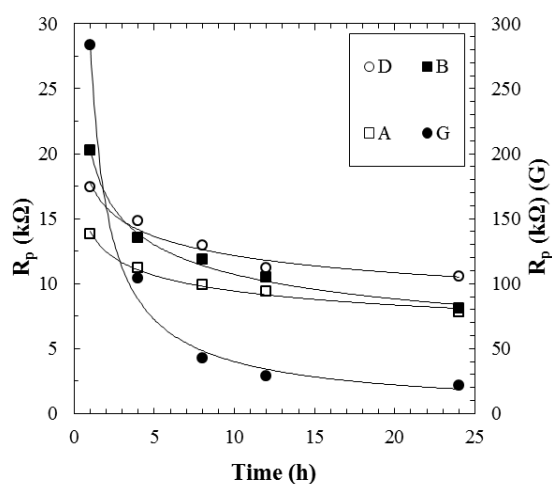
Fig. 7. Changes of polarization resistance (R_p) values of scratched coatings, 1-, 4-, 8-, 12- and 24 hours after immersion in 0.5 M NaCl solution. A, B, D and G samples are the coatings with no capsules (A, □), capsules with LO (B, ■), capsules with LO + 1 v/v% Co-octoate (D, ○) and capsules with LO + 2% ODA + 2 v/v% Co-octoate (G, ●), respectively.

Resistance of A, B and D samples are in the range of 7–17 kΩ after 1 h. The weakest coating was the reference. The barrier property of the paint can be enhanced by adding LO (B). In this case, drying of LO raises the resistance of the coating (D). These values are represented on the left 'y' axis. Although the visual observation did not show significant difference between coaintgs (D) and (G) in the period of 1-4 days, EIS measurements prove that in the first 24 h the sample (G) shows superior perfomrance to the others, with its R_p curve running one magnitude higher in the first several hours.

4. Summary

Microcapsules were prepared with the same shell material but with different core compositions of LO. In order to elucidate what will happen when LO is the main component in the core, its drying process was first in the focus of our work. The solidificaiton of LO film − either alone or in combination with additives like the siccative Co-octoate and the inhibitor ODA - was followed by FTIR technique and the most important bands, representing the oxydation reactions of the double bonds in the LO, were determined.
It turned out that because of special chemical reactions of the double bonds, the Co-octoate can significantly decrease the drying time of the LO. On the other hand, the presence of the ODA in the LO elongates that time. But when the siccative and the inhibitor are dissolved parallel in the LO film, the solidification time of the film decreases. This knowledge helped us in preparation of the microcapsules filled with different compositions.
These microcapsules were embedded into paints and their film forming and anticorroison activity were tested. Corrosion tests were run with commercial coatings containing LO-based microcapsules.
Based on the results, the difference between the barrier effect of the liquid and solid state LO is remarkable. Though LO has barrier properties even as liquid, for the quick recovery of a damage, it is necessary to use driers in the oil. To improve the self-healing activity, octadecylamine was encapsulated together with the LO. After compensating its drying impeder effect, the coating showed higher electrochemical resistance than the coatings without or with only LO-containing microcapsules.

5. Acknowledgements

6. References

[1] A. Stankiewicz, I. Szczygieł, B. Szczygieł, J. Mater. Sci. 48 (2013) 8041–8051.

[2] M.F. Montemor, Surf. Coat. Technol. (2014),
http://dx.doi.org/10.1016/j.surfcoat.2014.06.031

[3] J. Carneiro, J. Tedim, S.C.M. Fernandes, C.S.R. Freire, A.J.D. Silvestre, A. Gandini, M.G.S. Ferreira, M.L. Zheludkevich, Prog. Org. Coat. 75 (2012) 8–13.

[4] M.F. Montemor, M.G.S. Ferreira, Prog. Org. Coat. 63 (2008) 330–337.

[5] D. Snihirova, S.V. Lamaka, M. Taryba, A.M. Salak, S. Kallip, M.L. Zheludkevich, M.G.S. Ferreira, M.F. Montemor, ACS Appl. Mater. Interfaces 2 (2010) 3011–3022.

[6] D. Snihirova, S.V. Lamaka, M.F. Montemor, Electrochim. Acta 83 (2012) 439–447.

[7] M.F. Montemor, D.V. Snihirova, M.G. Taryba, S.V. Lamaka, I.A. Kartsonakis, A.C. Balaskas, G.C. Kordas, J. Tedim, A. Kuznetsova, M.L. Zheludkevich, M.G.S. Ferreira, Electrochim. Acta 60 (2012) 31–40.

[8] M. Plawecka, D. Snihirova, B. Martins, P.Warszynski, M.F. Montemor, Electrochim. Acta (2014), http://dx.doi.org/10.1016/j.electacta.2014.04.035.

[9] G.L. Li, Z. Zheng, H. Möhwald, D.G. Shchukin, ACS Nano 7 (2013) 2470–2478.

[10] D. Borisova, H. Möhwald, D.G. Shchukin, ACS Nano 5 (2011) 1939–1946.

[11] M.L. Zheludkevich, R. Serra, M.F. Montemor, M.G.S. Ferreira, Electrochem. Commun. 7 (2005) 836–840.

[12] M.L. Zheludkevich, D.G Shchukin, K.A. Yasakau, H. Möhwald, M.G.S. Ferreira, Chem. Mater. 19 (2007) 402–411.

[13] S.H. Boura, M. Peikari, A. Ashrafi, M. Samadzadeh, Prog. Org. Coat. 75 (2012) 292–300.

[14] M.W. Keller, S.R. White, N.R. Sottos , Adv. Funct. Mater. 17 (2007) 2399–2404 .

[15] M. Behzadnasab, M. Esfandeh, S.M. Mirabedini, M.J. Zohuriaan-Mehr, R.R. Farnood, Colloid Surface A 457 (2014) 16–26.

[16] C. Suryanarayana, K.C. Rao, D. Kumar, Prog. Org. Coat. 63 (2008) 72–78.

[17] T. Szabó, L. Molnár-Nagy, J. Bognár, L. Nyikos, J. Telegdi, Prog. Org. Coat. 72 (2011) 52–57.

[18] S.M. Mirabedini, I. Dutil, R.R. Farnood, Colloid Surface A 394 (2012) 74–84.

[19] T. Nesterova, K. Dam-Johansen, L.T. Pedersen, S. Kiil, Prog. Org. Coat. 75 (2012) 309–318.

[20] A. Pilbáth, T. Szabó, J. Telegdi, L. Nyikos, Prog. Org. Coat. 75 (2012) 480–485.

[21] M. Samadzadeh, S.H. Boura, M. Peikari, A. Ashrafi, M. Kasiriha, Prog. Org. Coat. 70 (2011) 383–387.

[22] X. Liu, H. Zhang, J. Wang, Z. Wang, S. Wang, Surf. Coat. Tech. 206 (2012) 4976–4980.

[23] S.J. García, H.R. Fischer, P.A. White, J. Mardel, Y. González-García, J.M.C. Mol, A.E. Hughes, Prog. Org. Coat. 70 (2011) 142–149.

[24] X. He , X. Shi, Prog. Org. Coat. 65 (2009) 37–43 .

[25] C.M. Dry, N. Sottos, in: K. Varadian (Ed.), Smart Structures and Materials 1995, Smart Materials, Proc. SPIE, 1916, 1993, pp. 438–444.

[26] S.R. White, N.R. Sottos, P.H. Geubelle, J.S. Moore, M.R. Kessler, S.R. Sriram, E.N. Brown, S. Viswanathan, Nature 409 (2001) 794–797.

[27] E.N. Brown, M.R. Kessler, N.R. Sottos, S.R. White, J. Microencapsul. 20 (2003) 719–730.

[28] S.H. Cho, S.R. White, P.V. Braun, Adv. Mater. 21 (2009) 645–649.

[29] X.-M. Tong, T. Zhang, M.-Z. Yang, Q. Zhang, Colloid Surface A 371 (2010) 91–97.

[30] N. Selvakumar, K. Jeyasubramanian, R. Sharmila, Prog. Org. Coat. 74 (2012) 461–469.

[31] E.W. Brooman, Met. Finish 100 (2002) 42–53.

[32] H. Choi, Y.-K. Song, K.Y. Kim, J.M. Park, Surf. Coat. Tech. 206 (2012) 2354–2362.

[33] J.M. Falcón, F.F. Batista, I.V. Aoki, Electrochim. Acta 124 (2014) 109–118.

[34] H. Choi, K.Y. Kim, J.M. Park, Prog. Org. Coat. 76 (2013) 1316–1324.

[35] H.H. Ge, G.-D. Zhou, Q.-Q. Liao, Y.G Lee, B.H. Loo, Appl. Surf. Sci. 156 (2000) 39–46.

[36] A. Rohani-Rad, J. Mofidi, Z. Modaress-Tehrani, Corros. Eng. Sci. Technol. 38 (2003) 79-80.

[37] B. Fan, G. Wei, Z. Zhang, N. Qiao, Corr. Sci. 83 (2014) 25–35.

[38] B.A. Boukamp, Solid State Ionics 20 (1986) 31–44.

[39] M. Lazzari, O. Chiantore, Polym. Degrad. Stabil. 65 (1999) 303–313.